

CHANGGYUN KIM¹, SEO YOUNG AN¹, HAN JANG¹, INJOON SON^{1*}

ENHANCEMENT OF EXOTHERMIC CHARACTERISTICS THROUGH NICKEL DISPLACEMENT PLATING ON ALUMINUM POWDER DEPENDING ON PH AND PARTICLE SIZE VARIABLES

Aluminum (Al) powders are attractive fuel additives for energetic materials, but their native Al_2O_3 shell suppresses exothermic reactivity. Here, we replace this oxide layer with a nickel (Ni) coating produced by displacement plating. After HF-based etching to strip the oxide, Ni was deposited at pH 9-12 and characterized by FE-SEM/EDS. Then, we tested Nickel displacement coverage on Aluminum powders with three different sizes ($\bar{d} \approx 10, 34, 68 \mu\text{m}$, respectively). We further quantified the exothermic heat release of bare and Nickel-coated Aluminum powders as a function of pH and particle size. Our results show that Nickel-coated Aluminum powders release substantially more heat (exothermic energy) than their bare counterparts, an increase attributed to a self-propagating high-temperature synthesis (SHS) reaction between Aluminum and Nickel. Finally, we compared how the coating morphology evolves with time when Ni is applied by displacement plating versus electroless plating.

Keywords: Aluminum (Al) powder; Nickel (Ni) displacement plating; Self-propagating high-temperature synthesis (SHS); pH, Size

1. Introduction

Metal powders possess a significantly larger surface area compared to their bulk counterparts, rendering them more reactive and, consequently, more explosive. As a result, metal powders have gained increasing attention for use in explosives and rocket propellants in recent years. Among various metal powders, aluminum (Al) is particularly attractive due to its high energy density and excellent thermal conductivity, making it an effective energetic material [1]. However, the presence of a naturally formed passivation layer of aluminum oxide (Al_2O_3) on the particle surface inhibits its reactivity. To overcome this limitation, recent studies have focused on enhancing the explosiveness of Al powders by removing the oxide layer and coating the particles with reactive metals or polymers [2,3]. Notably, when a metal coating is applied to aluminum powder, a phenomenon known as self-propagating high-temperature synthesis (SHS) can occur near the melting point of aluminum, leading to rapid energy release during ignition [4]. Displacement plating is a technique that exploits the difference in reduction potentials between two metals, enabling the spontaneous deposition of one metal onto another. Since nickel (Ni, -0.25 V) has a higher reduction potential than aluminum (-1.66 V), Ni can be deposited onto Al powder

through a displacement reaction. In this study, the native oxide layer on Al powders was removed through chemical etching, and displacement Ni plating was conducted under varying pH conditions and Al particle sizes. The resulting Ni-coated Al powders exhibited enhanced exothermic reactivity, which is attributed to the SHS reaction between Al and Ni at elevated temperatures.

2. Experimental

2.1. Sample fabrication

In this study, displacement nickel plating was performed using 5 g of aluminum (Al) powder with average particle sizes of 10, 34, and 68 μm . To remove the native oxide layer (Al_2O_3) from the powder surface, an etching process was carried out by stirring the Al powder in a solution of deionized (DI) water and 68% hydrofluoric acid (HF) for 2 minutes. The etched powder was then filtered and thoroughly rinsed with DI water to eliminate residual HF. Subsequently, the cleaned Al powder was introduced into a pre-prepared displacement nickel plating bath maintained at 40°C and stirred at 150 rpm for 30 minutes. The plating solution contained 30 g/L nickel sulfate ($\text{NiSO}_4 \cdot 6\text{H}_2\text{O}$),

¹ KYUNGPPOOK NATIONAL UNIVERSITY, SCHOOL OF MATERIALS SCIENCE AND ENGINEERING, DEPARTMENT OF MATERIALS SCIENCE AND METALLURGICAL ENGINEERING, KOREA

* Corresponding author: ijson@knu.ac.kr



50 mL/L ammonium hydroxide (NH_4OH , 25%), and 50 g/L ammonium citrate ($\text{NH}_4\text{C}_6\text{H}_5\text{O}_7$). The solution pH was adjusted to 8, 9, 10, 11, or 12 using NaOH. After plating, the powder was filtered and washed with DI water using a vacuum-assisted filtration device. The resulting powder was dried in a vacuum oven at 100°C for 24 hours to obtain the final product. For comparison, electroless nickel coating was also performed using a commercially available LSF solution.

2.2. Sample analysis

A field emission scanning electron microscope (FE-SEM, JSM-IT700HR, JEOL, Japan) was employed to examine the surface and cross-sectional microstructures of the Ni-coated aluminum powders. The morphology and surface coverage of the Ni coating were evaluated based on the SEM images. Additionally, energy-dispersive spectroscopy (EDS) was conducted to analyze the elemental composition of the coating layer, confirming the presence and distribution of nickel. To assess the exothermic reactivity of the plated aluminum powders, thermogravimetric-differential scanning calorimetry (TGA–DSC, SDT 650, TA Instruments, USA) was performed. The oxidation temperature and total heat release were quantitatively compared across samples with different pH conditions and aluminum particle sizes.

3. Results and discussion

3.1. pH-dependent physical and exothermic properties of displacement Ni-coated Al powders

Fig. 1 shows the SEM and EDS images of bare Al and displacement Ni-coated Al powders prepared under different pH conditions. According to the Pourbaix diagram of aluminum, a passive oxide film forms at pH levels below 8, which hinders the displacement Ni coating process [5]. This is consistent with the EDS image at pH 8 (Fig. 1b), where minimal Ni coverage

is observed, indicating that displacement Ni plating is ineffective under these conditions. As the pH increases, Ni deposition improves, with the highest Ni coverage observed at pH 10 (Fig. 1d) and pH 11 (Fig. 1e). This is attributed to the reduced extent of Al passivation compared to that at pH 8. Additionally, Al_2O_3 dissolves into $\text{Al}(\text{OH})_4^-$ in alkaline conditions, facilitating the reduction of Ni^{2+} ions onto the Al powder surface. However, at pH values above 12, Ni^{2+} begins to precipitate as $\text{Ni}(\text{OH})_2(\text{s})$, which hinders the reduction of Ni onto the Al powders. Fig. 2 illustrates the heat release profiles of raw Al powder and Ni-coated Al powders prepared under different pH conditions. Two distinct exothermic peaks are observed. The first peak appears around 660°C , corresponding to the melting point of aluminum. A similar thermal event was reported by Školáková et al. in their study on Ni–Al alloy sintering, where it was attributed to interdiffusion between Al and Ni in the vicinity of the Al melting point [6]. The second peak, observed near 1000°C , is ascribed to the self-propagating high-temperature synthesis (SHS) reaction between molten Al and solid Ni. During the SHS process, the high-temperature reaction between Al and Ni yields various intermetallic compounds, primarily AlNi, along with phases such as AlNi_3 , Al_3Ni_2 , and Al_3Ni_5 [7]. The molar enthalpy of formation for the predominant product, AlNi, during SHS has been reported as -127.2 kJ/mol, indicating a strong exothermic reaction [8]. Fig. 3 illustrates the SHS reaction process between Al and Ni. The energy released during this process is influenced by two key factors. First is the Ni coverage on the Al surface, which determines the number of available reaction sites. Second is the diffusion distance of molten Al, which governs the rate at which Al can migrate to the outer Ni layer and participate in the reaction. Additionally, a weight increase was observed at the temperatures corresponding to the first and second exothermic peaks. This phenomenon is attributed not only to the Ni–Al reaction but also to the formation of an Al oxide layer. Across all pH conditions, the heat released from the self-propagating high-temperature synthesis (SHS) reaction was greater than that from solid-state interdiffusion between Al and Ni. This can be explained by the higher diffusivity of liquid Al compared to solid Al, as well

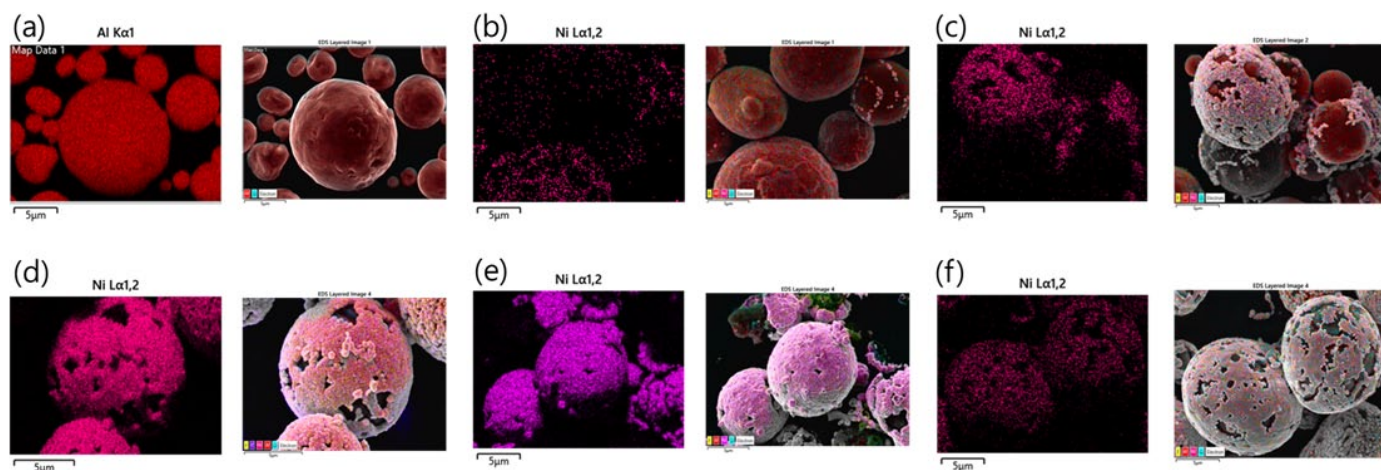


Fig. 1. EDS images of Ni plated 10 μm -diameter Al powder with different pH. (a) Raw Al powder, (b) Ni plated Al powder at pH 8, (c) Ni plated Al powder at pH 9, (d) Ni plated Al powder at pH 10, (e) Ni plated Al at pH 11, (f) Ni plated Al at pH 12

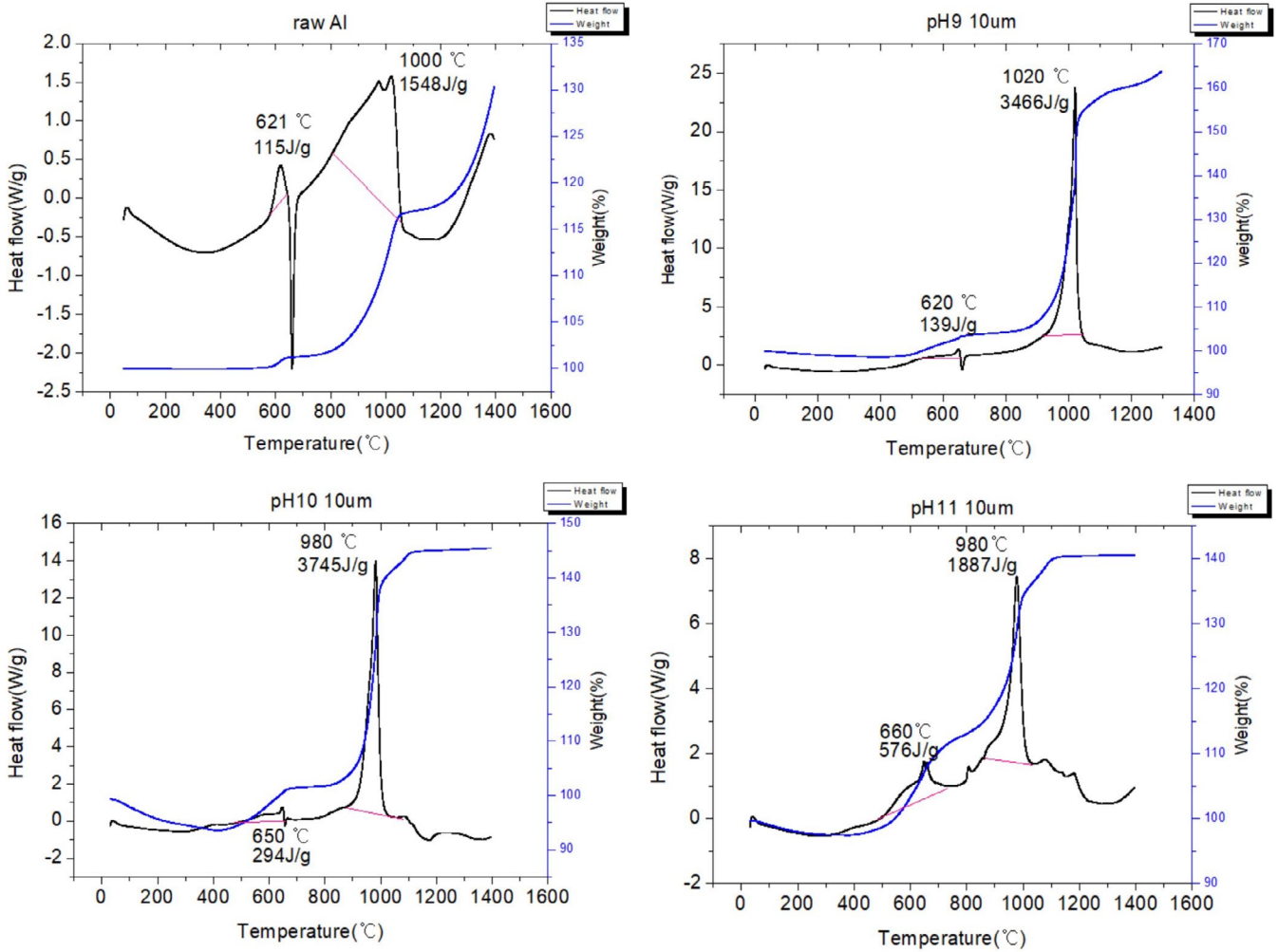


Fig. 2. TGA-DSC curves of Ni plated 10 um-sized Al powder with different pH (a) Raw Al powder, (b) Ni plated Al powder at pH 9, (c) Ni plated Al powder at pH 10, (d) Ni plated Al powder at pH 11

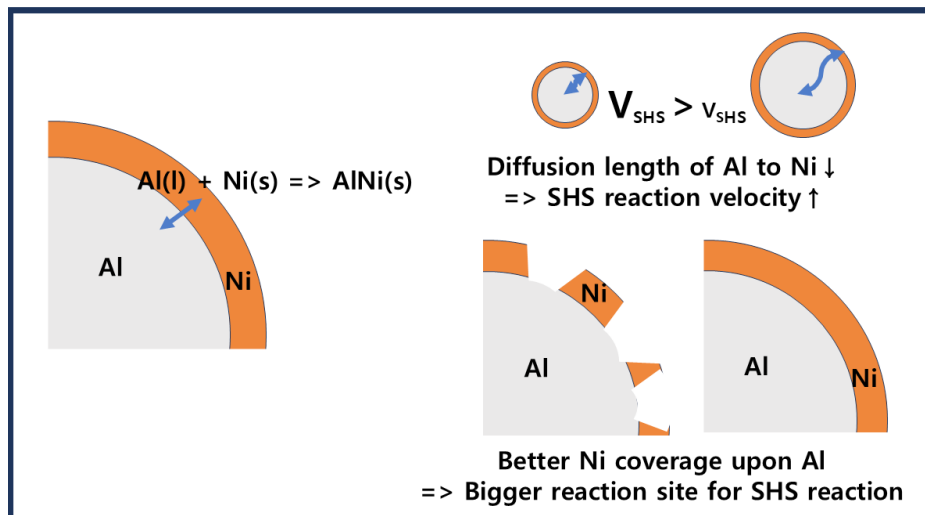


Fig. 3. Scheme depicting SHS reaction between Al and Ni

as the increased interfacial area in the liquid state, both of which facilitate the formation of intermetallic compounds (IMCs) between Al and Ni [9]. The total heat release, calculated as the sum of the first and second exothermic peaks, was highest for the

sample displacement-coated at pH 10 (Fig. 2c). As confirmed in the EDS images, Ni coverage was also greatest at pH 10, which correlates with the enhanced interdiffusion between Al and Ni under these conditions.

3.2. Size-dependent physical and exothermic properties of displacement Ni-coated Al powders

Fig. 4 presents the EDS mapping results of displacement Ni coating on Al powders with different particle sizes under pH 10 conditions. For Al powders with average particle sizes of 10 μm (Fig. 4a) and 34 μm (Fig. 4b), a high degree of Ni coverage was observed. In contrast, the 68 μm powder (Fig. 4c) exhibited partial regions with no Ni coating. This behavior is attributed to the larger specific surface area of smaller particles, which increases the likelihood of Ni ions in solution reacting with the Al surface. Similar trends were also reported by W.J. Iley et al., who demonstrated that smaller particle sizes facilitate the displacement plating process more effectively [10]. Fig. 5 presents the TGA–DSC curves for displacement Ni-coated Al powders with different average particle sizes under pH 10 conditions. As previously observed in the EDS analyses of displacement-coated samples at varying pH levels, Ni coverage correlates strongly with exothermic energy. Notably, the 10 μm Al powder exhibited the highest first and second exothermic peaks, as well as the greatest total heat release (Fig. 5a). This trend is attributed to the enhanced Ni coverage on smaller Al particles during displacement plating, which increases the interfacial area available for Al–Ni interdiffusion reactions. In addition, particle diameter can be regarded as a diffusion path length for Al atoms migrating from the particle core to the Ni-coated surface. According to the spherical diffusion model, diffusion time is proportional to the square of the diffusion distance ($t \propto R^2$). Therefore, Al atoms in 10 μm particles reach the Ni interface more rapidly than in larger particles, thereby facilitating faster and more extensive interfacial reactions [11].

placement plating, which increases the interfacial area available for Al–Ni interdiffusion reactions. In addition, particle diameter can be regarded as a diffusion path length for Al atoms migrating from the particle core to the Ni-coated surface. According to the spherical diffusion model, diffusion time is proportional to the square of the diffusion distance ($t \propto R^2$). Therefore, Al atoms in 10 μm particles reach the Ni interface more rapidly than in larger particles, thereby facilitating faster and more extensive interfacial reactions [11].

3.3. Time-dependent morphological evolution of displacement and electroless Ni coatings on Al powder

Fig. 6 illustrates the morphological evolution of Al powder over time when coated via displacement Ni plating and electroless Ni plating. In displacement Ni plating, Ni deposits on the Al powder in a cotton-like morphology (Fig. 6a), whereas in electroless Ni plating, Ni forms discrete, spherical particles on the surface (Fig. 6b). Unlike the electroless process, which produces isolated Ni particles, displacement Ni plating yields a continuous, fibrous Ni layer. This interconnected structure

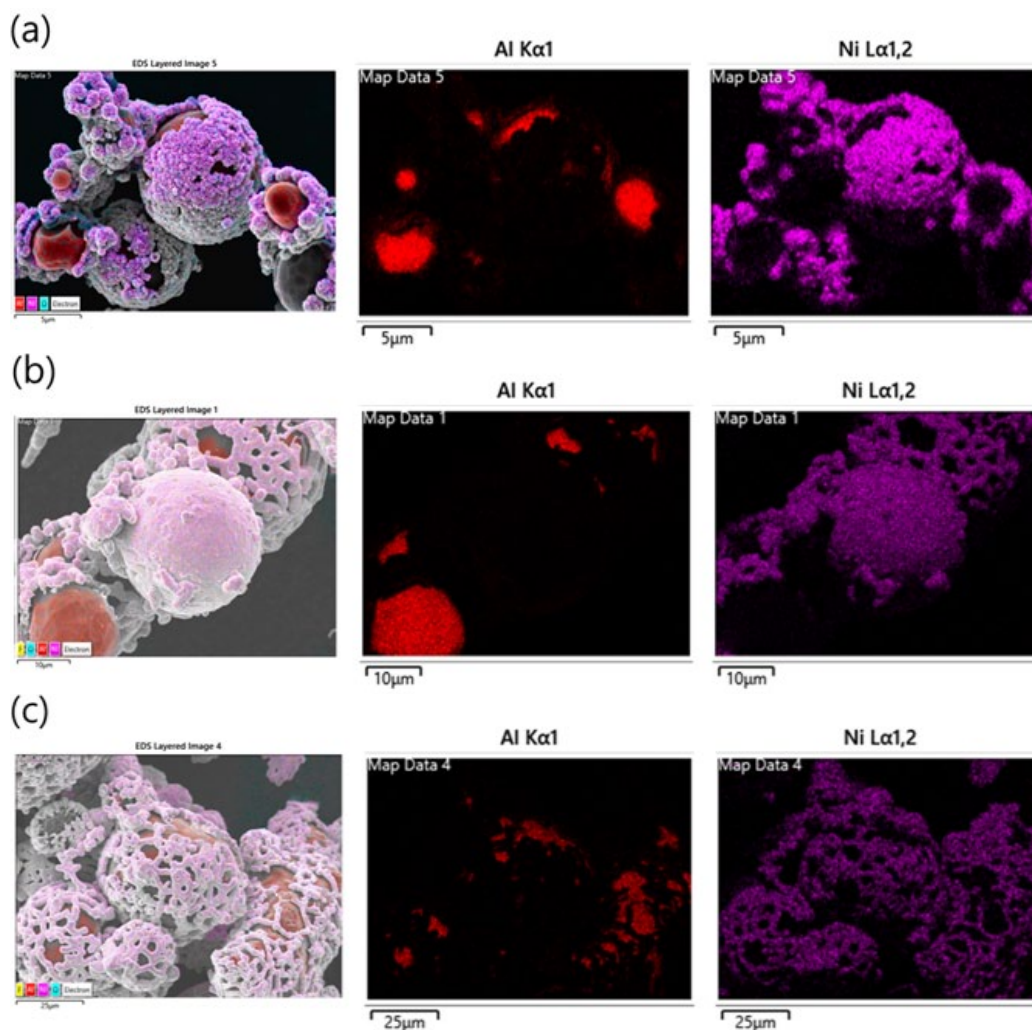


Fig. 4. EDS images of Ni plated Al powder at pH 10 with different powder size. (a) Average Powder size 10 μm , (b) Average Powder size 34 μm , (c) Average Powder size 68 μm

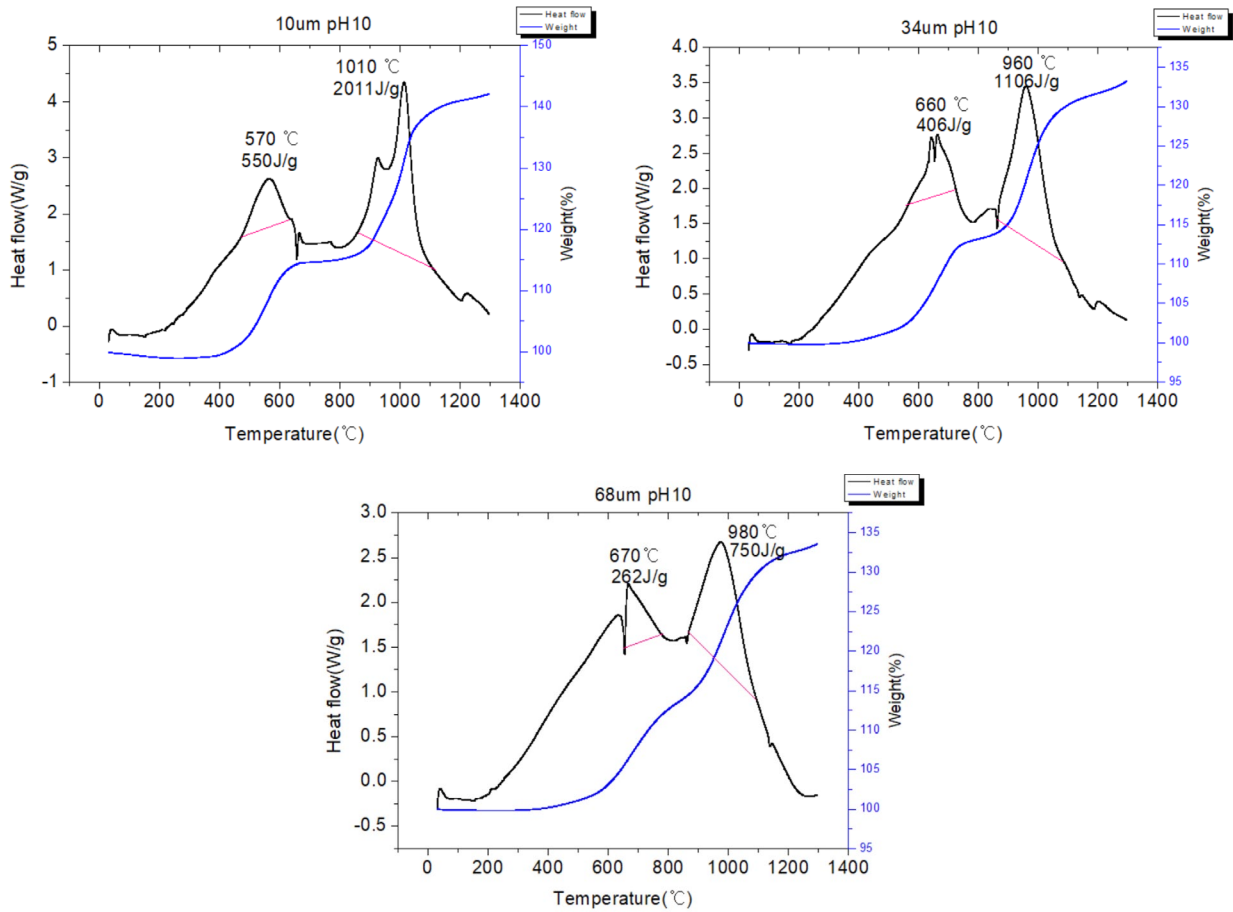


Fig. 5. TGA-DSC curves of Ni plated Aluminum powder at pH 10 with different powder sizes. (a) Average Powder size 10 um, (b) Average Powder size 34 um, (c) Average Powder size 68 um

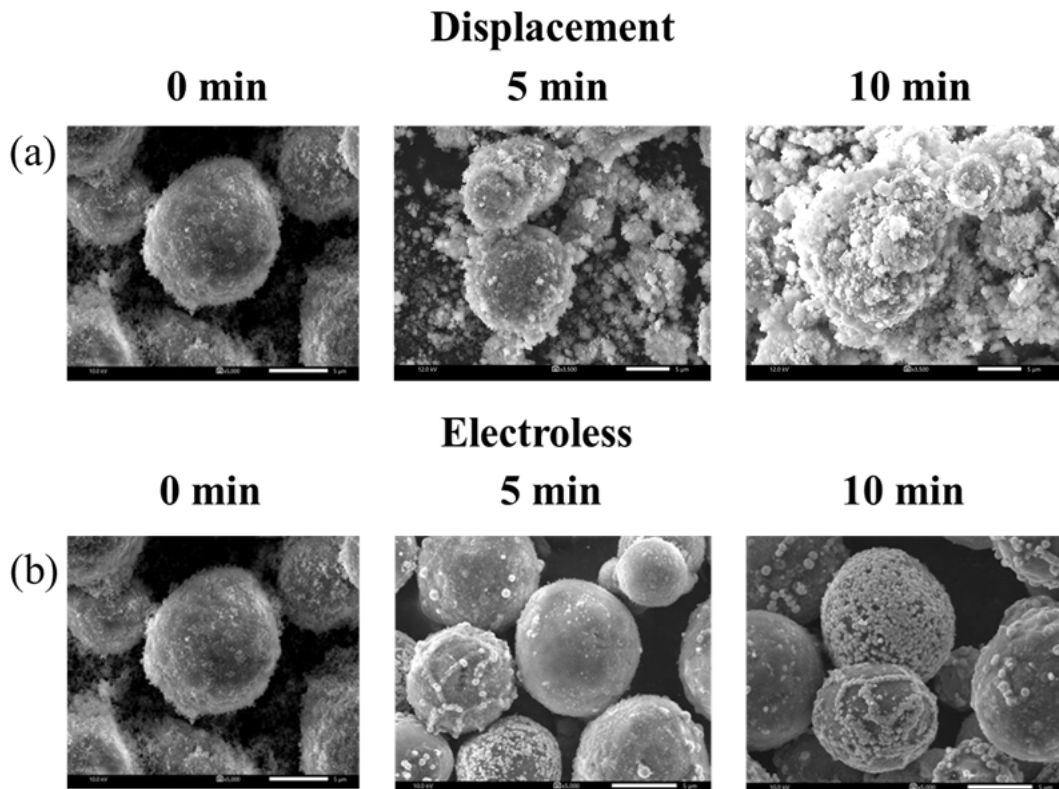


Fig. 6. Morphology changes of Ni plated (Electroless VS Displacement) Al with plating time elapsed. (a) Displacement Ni plated Al powders with time (0~10 min), (b) Electroless Ni plated Al powders with time (0~10 min)

provides more efficient diffusion pathways, thereby enhancing the Ni–Al interfacial reaction. Notably, the Ni particles formed by displacement plating are smaller in size compared to those produced by electroless plating. Furthermore, after 10 minutes of plating, the surface coverage of Ni on Al powder is significantly higher in the displacement method. This increased Ni coverage results in a larger interfacial contact area between Ni and Al, which, in turn, leads to an expanded reaction interface during the Ni–Al self-propagating high-temperature synthesis (SHS) process.

4. Conclusion

In this study, a displacement Ni plating method was employed to compare and analyze the extent of Ni coating as a function of pH and Al powder particle size. The results were further correlated with the exothermic behavior of the Ni-coated Al powders.

REFERENCES

- [1] L. Meda, G. Marra, L. Galfetti, F. Severini, L. De Luca, Nano-aluminum as energetic material for rocket propellants. *Mater. Sci. Eng. C* **27** (5-8), 1393-1396 (2007). DOI: <https://doi.org/10.1016/j.msec.2006.09.030>
- [2] K.T. Kim, D.W. Kim, C.K. Kim, Y.J. Choi, A facile synthesis and efficient thermal oxidation of polytetrafluoroethylene-coated aluminum powders. *Mater. Lett.* **167**, 262-265 (2016). DOI: <https://doi.org/10.1016/j.matlet.2016.01.003>
- [3] K.T. Kim, D.W. Kim, S.H. Kim, C.K. Kim, Y.J. Choi, Synthesis and improved explosion behaviors of aluminum powders coated with nano-sized nickel film. *Appl. Surf. Sci.* **415**, 104-108 (2017). DOI: <https://doi.org/10.1016/j.apsusc.2016.11.056>
- [4] F. Baras, V. Turlo, O. Politano, S.G. Vadchenko, A.S. Rogachev, A.S. Mukasyan, SHS in Ni/Al nanofolios: a review of experiments and molecular dynamics simulations. *Adv. Eng. Mater.* **20** (8), 1800091 (2018). DOI: <https://doi.org/10.1002/adem.201800091>
- [5] G.D. Davis, W.C. Moshier, J.S. Ahearn, H.F. Hough, G.O. Cote, Corrosion/passivation of aluminum in dilute sulfate solutions: a comparison of Pourbaix and surface behavior diagrams. *J. Vac. Sci. Technol. A* **5** (4), 1152-1157 (1987). DOI: <https://doi.org/10.1116/1.574625>
- [6] A. Školáková, J. Körberová, P. Kratochvíl, P. Salvetr, D. Deduytsche, P. Novák, A comprehensive description of reactions between nickel and aluminum powders during reactive sintering. *Mater. Chem. Phys.* **271**, 124941 (2021). DOI: <https://doi.org/10.1016/j.matchemphys.2021.124941>
- [7] F.Z. Chrifi-Alaoui, M. Nassik, K. Mahdouk, J.C. Gachon, Enthalpies of formation of the Al–Ni intermetallic compounds. *J. Alloys Compd.* **364**, 121-126 (2004). DOI: [https://doi.org/10.1016/S0925-8388\(03\)00659-0](https://doi.org/10.1016/S0925-8388(03)00659-0)
- [8] C. Curfs, X. Turrillas, G.B.M. Vaughan, A.E. Terry, Å. Kvik, M.A. Rodríguez, Al–Ni intermetallics obtained by SHS; time-resolved X-ray diffraction study. *Intermetallics* **15**, 1163-1171 (2007). DOI: <https://doi.org/10.1016/j.intermet.2007.02.002>
- [9] K. Naplocha, Self-propagating high-temperature synthesis (SHS) of intermetallic matrix composites, in: R. Mitra (Ed.), *Intermetallic Matrix Composites: Properties and Applications*, Woodhead Publ. 203-220, Cambridge (2018). DOI: <https://doi.org/10.1016/B978-0-85709-346-2.00008-x>
- [10] W.J. Iley, Effect of particle size and porosity on particle film coatings. *Powder Technol.* **65** (1-3), 441-445 (1991). DOI: [https://doi.org/10.1016/0032-5910\(91\)80205-w](https://doi.org/10.1016/0032-5910(91)80205-w)
- [11] X. Ren, G. Chen, W. Zhou, C. Wu, J. Zhang, Formation and growth kinetics of intermediate phases in Ni–Al diffusion couples. *J. Wuhan Univ. Technol. Mater. Sci. Ed.* **24**, 787-790 (2009). DOI: [10.1007/s11595-009-5787-9](https://doi.org/10.1007/s11595-009-5787-9)